

Response to Interactive comment on “Evidence for an unidentified ground-level source of formaldehyde in the Po Valley with potential implications for ozone production” by J. Kaiser et al.

Anonymous Referee #1

We thank the referee for the valuable comments. The original comments are shown in italicized black, while responses are provided below in blue.

In this paper Kaiser et al have measured HCHO from the Zeppelin NT platform over the Po valley in Italy. The measurements are made using a highly sensitive in situ instrument based on LIF spectroscopy, and with good time resolution. The combination of this instrument and the Zeppelin platform enable some unique measurements to be made of HCHO in the first 1 km of the boundary layer. The main result from this paper is that the measurement cannot be reconciled with the results from a 1D model of the atmosphere without invoking a surface source emission of HCHO, and from an analysis of the vertical profile of HCHO, and the origin of the airmass, the authors, after ruling out several possibilities, conclude that agricultural emissions of HCHO from the surrounding countryside are responsible for the gap between measurements and models. There is good supporting suite of measurements on the Zeppelin which are used to help formulate this conclusion. Most of the discussion of the other measurements are in separate papers. There are some assumptions which have been used to make this conclusion, and which are discussed in the paper. The results are important as the Po valley is a notoriously polluted location, with ozone, which is formed as a result of further degradation of HCHO, being often above the EU exceedance limit value.

The results are not totally new, there was a previous study in this region in the FORMAT campaign, where HCHO was underestimated by a model, but the identification of the missing HCHO from local agricultural sources is new. Also in this study measurements of OH reactivity are available, which enable confidence to be gained that all the OH sinks are inputted into the model (i.e. that it is not a problem with missing OH sinks in the model which leads to an underestimate of the HCHO levels). An impact of the work is that additional ozone is generated from the missing HCHO. The paper is suitable for publication in ACP. But I would like to authors to consider the points below prior to publication in ACP.

Specific points

Page 25145. Line 2. Why is the precision varying over such a wide range (20-200 pptv?). Although it is related to the precision and the sensitivity of the instrument, it would be useful to state the range of limits of detection exhibited by the instrument during the campaign.

Precision derived from measurements of synthetic air is ~ 20 ppt in 1 s. For higher concentrations, precision is derived from the standard deviation of the measurement at a constant

concentration (~200 ppt at 3 ppb). Our empirical determination of precision does not deviate from what would be anticipated for a shot-noise limited detection scheme. The limit of detection is calculated from the precision of the measurements of synthetic air, and is now stated in the manuscript (2σ LOD = 40 ppt).

Page 25145. Line 18. MCM v3.2 is the most to date version of the MCM, but this update was given quite recently, and so Saunders et al., 2003 seems too old a reference to the MCM. Is there a more up to date reference which describes some of the changes in the MCM with version 3.2?

The reference has been changed to reflect the citation suggested on the MCM website. This includes the website url, so that the reader can reference the version used in this manuscript and any future alterations.

Some further justification of the NH background value of CH₄ used in the model is needed, even if it is to say there are no emissions of CH₄ anywhere close (e.g. from natural gas lines, extraction activity from fracking etc.).

As noted by the second referee, emissions from agriculture (rice paddies and livestock) and natural gas fields may lead to enhanced CH₄ in the Po Valley.

We have recently received measurements of CH₄ in the Po-Valley from a mobile aerosol and trace gas laboratory ("Measurements Of Spatial QUantitative Immissions of Trace gases and Aerosols": MOSQUITA; Bukowiecki et al., 2002; Mohr et al., 2011), which was equipped with a Picarro Cavity Ring-Down Spectroscopy instrument. MOSQUITA-based CH₄ measurements were acquired from 8 June 2012 to 9 July 2012 (Figure R1). While measurements are not available on the day used in these model simulations, the average measurement acquired in the flight region of the Zeppelin is likely applicable to this study. The average mixing ratio of 2355 ppb is higher than the global average of 1760 ppb initially used in the model.

Though the increased methane concentration has little impact on our analysis and no impact on our conclusions, all model runs presented in the manuscript now use the average MOSQUITA CH₄ measurement.

Line 8. Please state the % total of the OH reactivity which is from NO_x and CO, as this will provide a useful guide as the importance of the VOCs towards OH reactivity in this environment. Also, what % of the OH reactivity comes from HCHO itself? The MS only states that HCHO is the largest contributor from the VOCs.

The relative contributions of NO_x (41%), CO (13%), and all measured VOCs and OVOCs (26%, including HCHO which is 8%) to modeled OH reactivity in the boundary layer (100 m) at 8:45 AM are now included in the manuscript.

Page 25148. Line 24. "compared" and not "compare"

Corrected.

Page 25149. Given that this paper discusses quite a bit the sinks for OH via the OH reactivity measurements, and that HCHO levels are related to the concentration of HO₂, I was surprised not to see a discussion about the significant missing gas-phase source of HONO from HO₂ inferred from the Zeppelin measurements and reported earlier this year. Are these findings not relevant to this study in any way? I realise that most of this current paper is about the mixed layer close to the surface, whereas the Science paper was about missing HONO sources from HO₂ in the residual layer which was disconnected to the BL early in the morning, but some links to the other paper might be made?

Because the proposed mechanism forming HONO presented by Li et al. (2014) has not been confirmed, no additional gas-phase HONO formation mechanism is included in our model. While the source of HONO is uncertain, it is unlikely to affect analysis of the HCHO budget as HONO, OH, HO₂, and NO_x are constrained to measurements.

Page 25152. Line 20. Why did measured HO₂ have a large uncertainty? This has led the authors here not to compare HO₂ levels to a model, which is a shame, as a lot would have been learnt from this. In the Science paper earlier this year HO_x levels were compared to the model. Did the HO₂ measurements just have a larger uncertainty for this portion of the study?

Page 25152. Line 16. HCHO is responsible for about 45% of the HO₂ production, it is a shame that the measured HO₂ values could not be used, as there is clearly a critical link between HO₂ and HCHO. What was the uncertainty of the HO₂ measurements? Some discussion is needed otherwise the statement that the model runs produced HO₂ within the uncertainty of the measurements is not helpful. Not including all HCHO sources has significant effects on the modelled HO₂ concentrations (line 17), and so a discussion of measured/modelled HO₂ provides confidence in this earlier statement. Given that HO₂ dominates the production of O₃ (line 16) not being able to use the measured HO₂ is a weakness of the approach. Also consistency between measured HO₂ and HCHO would help to confirm that there are missing sources of HCHO in the model.

As described in the supplement of the Li et al. (2014), an NO related interference causes the HO₂ measurement to be positively offset. In the laboratory, the offset was measured to be $(0.7 \pm 0.2) \times 10^8$ molecules/cm³. In the field, the measured value varied between 1.7×10^8 and 3.9×10^8 molecules/cm³. The reported data is corrected using lab-based measurements, which may misrepresent the actual offset by as much as 3×10^8 molecules/cm³. The cause for the discrepancies in the measured offsets is unclear.

The reported accuracy for the HO₂ measurements (24-30%, 1σ) is based on the error and reproducibility of calibrations. Boundary layer measurements are as low as 1×10^8 molecules/cm³. Because the measurements are near the value of the offset, and because the uncertainty in the offset is as much as 3 times the measurement, there is limited value in

comparing measured and modeled HO₂. The difference in concentration of HO₂ between the two model scenarios is ~12%, which is smaller than the measurement uncertainty calculated from calibrations and nearly invisible when viewed alongside the uncertainty associated with the offset (Figure R2).

Because the HO₂ measurements cannot provide further quantitative insight into this analysis, we rely on the two modeled HO₂ scenarios discussed in the text. Alternatively, the reported HO₂ and modeled HO₂ (using modeled HCHO) could be used to calculate missing O₃ production. This leads to a much larger missing P(O₃), as the discrepancy in HO₂ concentrations between the two scenarios is then ~60%. Given the uncertainty in the HO₂ measurements, using two model scenarios is a more conservative and realistic depiction of the effect of HCHO sources on P(O₃).

The same flight data is used here as in Li et al. (2014). In that analysis, “observed” HO₂ + HO₂H₂O is higher than the modeled scenario, and this is attributed to an offset in HO₂ measurements (see caption of Figure 4). However, because the authors use modeled HO₂ + HO₂H₂O rather than the observations in their analysis, this does not influence their conclusions. Similarly, we use model HO₂ so that conclusions are not influenced by potential measurement issues.

Page 25159. It would be useful in the Table to make an explicit statement of the LODs which are related to the precision. For the Spectroradiometer entry in the table, it was not clear what the “-“ means?

Both the accuracy and precision of the measured J values are dependent on conditions and the photolysis process. Two examples of photolysis frequencies as examples are:

j(NO₂): LOD approx. 1×10^{-7} /s, accuracy approx. 5%

j(O¹D): LOD approx. 5×10^{-8} /s, accuracy approx. 10%

LODs are derived from nighttime measurements of a Zeppelin radiometer before and after the 2012 campaign. The 15% accuracy is a conservative “mean” for all photolysis frequencies because for some species photolysis quantum yields are poorly known.

The HCHO LOD is now explicitly stated in the manuscript.

The OH and HO₂ precisions currently listed in the table are given as the limit of detection.

For VOCs, precision and LOD is substance dependent. Substance-specific LODs are provided in the cited reference.

This leaves k_{OH}, HONO, NO_x, O₃, and CO. For these parameters, the LOD can be calculated from the precision reported in the table. This information is now clarified either by footnotes, available in the cited references, or stated within the text of the manuscript.

Page 25162. Figure 3. Base model and the other legend labels need some supporting statement in the caption, even if to refer to some text in the main body of the MS.

The caption has been altered to refer readers to the text for detailed model scenarios descriptions.

Page 25163. Figure 4. A plot of OH reactivity with altitude would be instructive here, as it is difficult to see the direct link between OH reactivity and altitude here. Also why are only data during the ascents included in the figure, this wasn't clear.

A plot of OH reactivity with altitude is given in Fig. 2 and Fig. 3.

Descents were performed ~3 times more quickly than ascents. Instruments with lower time resolution (i.e. VOCs) acquired only a few measurements during the descent, with each measurement representing a large vertical range. Because vertical spatial resolution is important to our analysis, we restrict ourselves to the data acquired during the ascents. This is now clarified in the manuscript.

Page 25164. Figure 5. I think the equations of the lines are not necessary on the figure. They detract from the clarity of the figure and the values do not make immediate sense in the context of the figure. There are no data after 1100 on the figure, so I didn't understand how a line could be fitted to data after 1100 ("top"). Add the word "line" to bottom, middle and top? This figure and the explanation is not that clear.

The figure has been altered to only show mixed layer measurements, and linear fits are removed. The caption now states the main point: There is little variation in mixed layer CO, and the correlation with HCHO is small ($r^2=0.29$).

Page 25165. Figure 6. Be clear in the caption that it is the difference in modelled O3 for HCHO (calculated) minus modelled O3 for HCHO (measured) (and not the other way around).

The caption has been reworded. Missing $P(O_3)$ is defined as $P(O_3)$ calculated using measured HCHO minus $P(O_3)$ calculated using modeled HCHO.

References

Bukowiecki, N., Dommen, J., Prévôt, A. S. H., Richter, R., Weingartner, E., and Baltensperger, U.: A mobile pollutant measurement laboratory – measuring gas phase and aerosol ambient concentrations with high spatial and temporal resolution, *Atmos. Environ.*, 36, 5569–5579, doi:10.1016/S1352-2310(02)00694-5, 2002.

Mohr, C., Richter, R., DeCarlo, P. F., Prévôt, A. S. H., and Baltensperger, U.: Spatial variation of chemical composition and sources of submicron aerosol in Zurich during wintertime using mobile aerosol mass spectrometer data, *Atmos. Chem. Phys.*, 11, 7465-7482, doi:10.5194/acp-11-7465-2011, 2011.

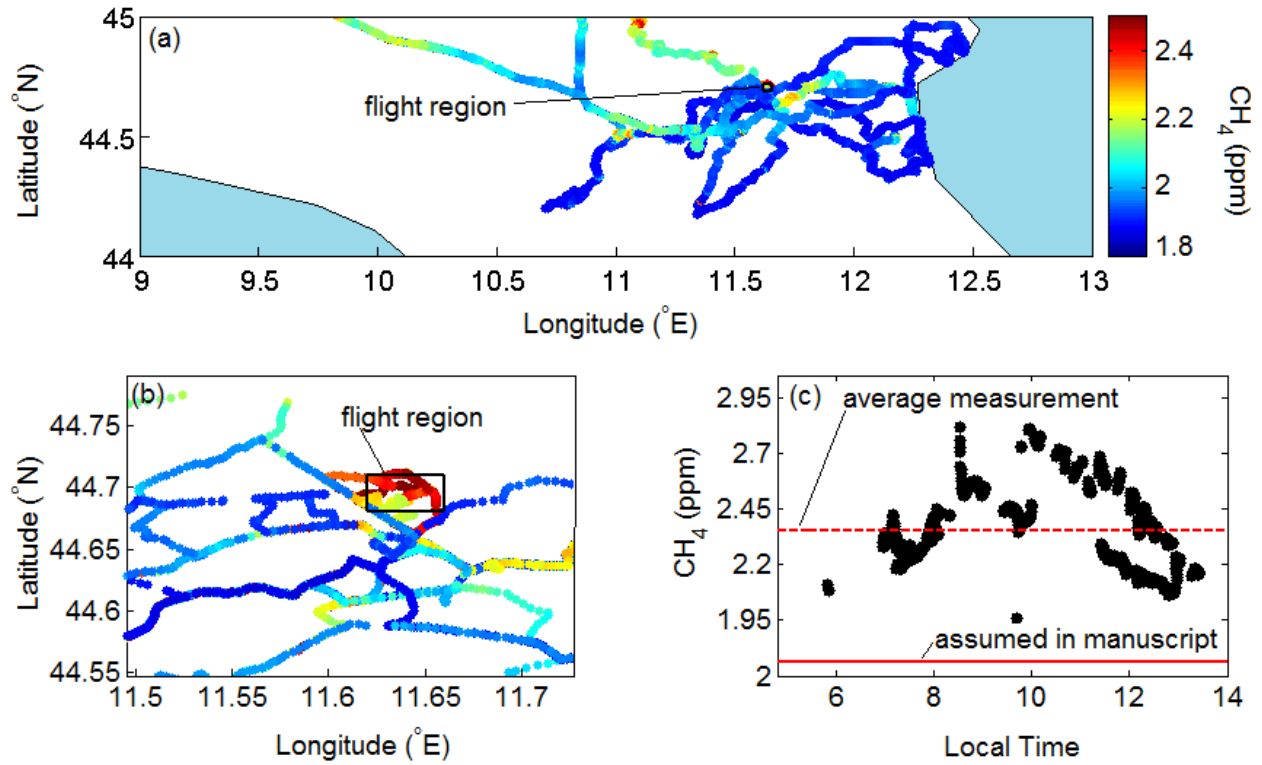


Figure R1. (a) Po-Valley methane measurements acquired from the MOSQUITA during PEGASOS 2012. (b) Zoomed in region highlighting the enhanced methane in the flight region. (c) Time series of methane measurements acquired in the boxed region of (b).

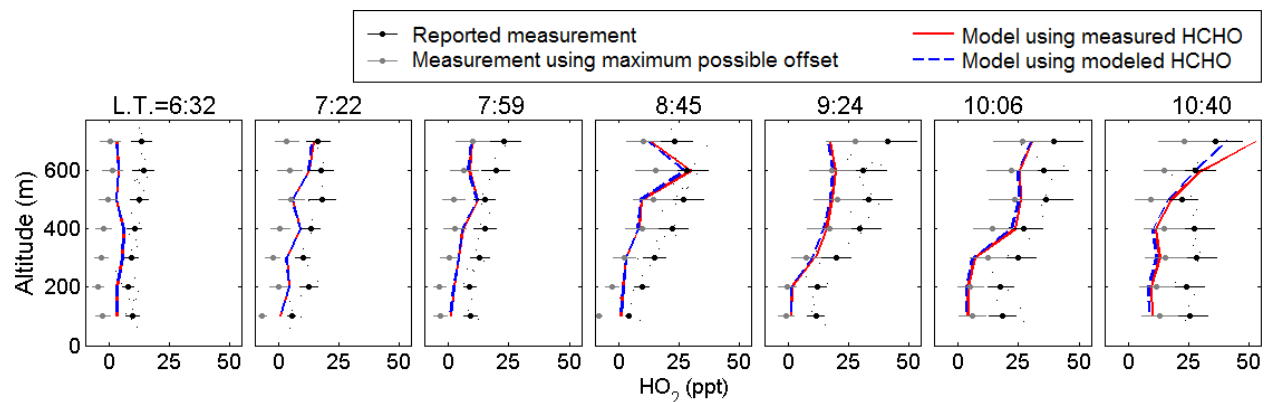


Figure R2. Reported HO₂ and the lower limit on HO₂ measurements based on the uncertainty in the measurement offset. Error bars represent a 30% 1 σ uncertainty. Modeled HO₂ concentrations refer to the two scenarios in the manuscript used to investigate missing P(O₃).

Response to interactive comment on “Evidence for an unidentified ground-level source of formaldehyde in the Po Valley with potential implications for ozone production” by J. Kaiser et al.

Anonymous Referee #2

We thank the referee for the valuable comments. The original comments are shown in italicized black, while responses are provided below in blue.

General remarks:

The manuscript describes detailed measurements of atmospheric trace gases taken within the planetary boundary layer from a Zeppelin airborne platform compared to a modeling study of air chemistry in the early morning hours. The measurements cover a wide range of chemical components compiled to constrain a direct comparison between model and experiment to identify possible gaps in our knowledge of sources and sinks of air chemistry or pollution relevant compounds. The paper is well structured and written in a concise way. It is made clear, that the model and experiment differ significantly in the concentrations of formaldehyde. However, the statement that the most probable source of missing HCHO is the direct emission from the soil and plant matter below the Zeppelin is not confirmed by the data given.

While we agree that we do not have unequivocal proof of direct emissions from soil and plant matter, our data does provide evidence of an unidentified ground-level source of formaldehyde, as stated in the manuscript title. Because measured and modeled OH reactivity are in good agreement, this additional source cannot be photochemical in nature. As direct emissions from anthropogenic sources are ruled out, and because agricultural activity in the surrounding area was high, soil and plant matter more likely than any other source of direct HCHO emission. Specific concerns are addressed below.

Specific comments:

Model simulations:

The model is using a global background concentration of methane, a precursor of formaldehyde (not measured from the Zeppelin, nor on the ground) of 1760 ppb. That is probably not realistic in the Po-Valley where major methane emissions are from agriculture (rice paddies and livestock). With the diurnal variation of the planetary boundary layer nighttime methane concentrations in agricultural areas could be far higher. (see for example www.gl.ethz.ch/news/Bamberger_etal.pdf). Such a variability of the methane, which is one of the precursors of formaldehyde in the Po valley, is not discussed but could affect also the early morning chemistry. Methane also provides a large fraction of the OH reactivity especially in the lowest layers (Fig.4). There are also other sources for methane in the vicinity of the SPC station

which could contribute to the diurnal variability and nighttime enhancements below the nocturnal inversion. Within the Po-valley there are at least 50 natural gas fields, several very close to SPC. It should be discussed how such variable methane concentrations affect the model results.

We have recently received measurements of CH₄ in the Po-Valley from a mobile aerosol and trace gas laboratory ("Measurements Of Spatial QUantitative Immissions of Trace gases and Aerosols": MOSQUITA; Bukowiecki et al., 2002; Mohr et al., 2011), which was equipped with a Picarro Cavity Ring-Down Spectroscopy instrument. MOSQUITA-based CH₄ measurements were acquired from 8 June 2012 to 9 July 2012 (Figure R1). While measurements are not available on the day used in these model simulations, the average measurement acquired in the flight region of the Zeppelin is likely applicable to this study. The average mixing ratio of 2355 ppb is higher than the global average of 1760 ppb initially used in the model.

We have repeated the base-case scenario using the average of the MOSQUITA measurements. Results are shown in Figure R2. The effect of CH₄ on modeled OH reactivity and HCHO is negligible. The model scenario using high concentrations of ethene show that modeled and measured HCHO and OH reactivity cannot be brought into agreement by adding any photochemical HCHO precursor. Because ethene has a higher yield of HCHO per OH reactivity, the model scenario currently presented in the manuscript addresses the concern of photochemical HCHO production more fully than a model scenario with increased CH₄.

Though the increased methane concentration has little impact on our analysis and no impact on our conclusions, all model runs presented in the manuscript now use the average MOSQUITA CH₄ measurement.

Model sensitivity to turbulent mixing (supplement): This discussion shows the variable eddy diffusion is not changing the results. This discussion could be shortened in case, the model can be constrained to the measured 3D wind –measurements (page 25145, line 12).

The SCM has actually been constrained with 3D wind fields but not those measured by the Zeppelin. The reason not to use the Zeppelin 3-D wind field observations is that they only cover a limited timeframe of the simulations covering multiple days. Alternatively, for studies with the SCM in support of analysis of observations such as those collected in the PEGASOS campaign we generally use the ECMWF re-analysis data to consider the role of advection and changes in synoptic conditions. This generally results in a quite realistic simulation of the actual meteorological conditions encountered during the campaign. However, we wanted to assess the sensitivity of the simulated reactive compound concentrations to turbulent transport being key to boundary layer exchange of tracers with lifetimes such as HCHO and its precursors. We feel the supplemental information provides useful information justifying the assumptions made in the manuscript (particularly, that the vertical mixing is accurately represented in the model

framework, and that reflective boundary conditions are appropriate). Because the discussion is in the supplement, it does not distract from the text.

Potential sources of HCHO: page 25149 line 16 to 29. A source region of Bologna (southwest of SPC) could be more simply excluded using a HYSPLIT backtrajectory, and on line wind measurements onboard the Zeppelin. A backtrajectory analysis could also help to investigate whether other sources of HCHO (or CH₄?, or biofuel) could possibly be located upwind of SPC.

As discussed above, we can exclude photochemical sources of HCHO such as biofuel and methane. This leaves the possibility that HCHO is transported from a source region with high HCHO. The main wind direction was from W to WNW; wind speeds were generally low between 0 and 6 m/s (Fig. R3). The manuscript does not state that transport from Bologna is impossible, but that only 90 ppt (7% of the missing HCHO) can be accounted for if the air is transported from Bologna.

To determine if Bologna or other source regions can be excluded as potential HCHO sources, an ensemble of 4-hour and 12-hour kinematic back trajectories (BTs) were calculated using the HYbrid Single-Particle Lagrangian Integrates Trajectory (HYSPLIT) model (Draxler and Rolph, 2003), initializing at each hour, and ending at the approximate time and location of the observed rise in HCHO (44.695°N, 11.64°E, 300 m asl, 7 UTC). The Global Data Assimilation System archive was used for meteorological inputs.

Because there is large variability in the calculated back trajectories, HYSPLIT analysis neither excludes nor highlights potential sources of advected HCHO, including Bologna (Figure R4 and R5). For this reason, and because the analysis currently presented in the manuscript places an upward bound on the potential role of advection, we do not feel it would benefit the manuscript to include HYSPLIT outputs.

Implications for ozone production: Are there any ground based ozone measurements available at SPC that could be use to confirm the model? How do they agree with ozone measurements from the Zeppelin?

In the calculations for ozone production rates, ozone mixing ratios are constrained to the measured values. Calculations of ozone mixing ratios or O₃ vertical structure depend on chemical and physical processes that are beyond the scope of this paper.

printing errors in the supplement page 3, line 17, remove ..as..

Corrected.

page 4, line 6: significantly

Corrected.

Acknowledgements

The authors gratefully acknowledge the NOAA Air Resources Laboratory (ARL) for the provision of the HYSPLIT transport and dispersion model used in this publication.

References

Bukowiecki, N., Dommen, J., Prévôt, A. S. H., Richter, R., Weingartner, E., and Baltensperger, U.: A mobile pollutant measurement laboratory – measuring gas phase and aerosol ambient concentrations with high spatial and temporal resolution, *Atmos. Environ.*, 36, 5569–5579, doi: 10.1016/S1352-2310(02)00694-5, 2002.

Draxler, R. R. and Rolph, G. D.: HYSPLIT (HYbrid Single-Particle Lagrangian Integrated Trajectory) Model access via NOAA ARL READY Website, NOAA Air Resour. Lab., Silver Spring, Md., available online at: <http://www.arl.noaa.gov/ready/hysplit4.html>, 2003.

Mohr, C., Richter, R., DeCarlo, P. F., Prévôt, A. S. H., and Baltensperger, U.: Spatial variation of chemical composition and sources of submicron aerosol in Zurich during wintertime using mobile aerosol mass spectrometer data, *Atmos. Chem. Phys.*, 11, 7465-7482, doi:10.5194/acp-11-7465-2011, 2011.

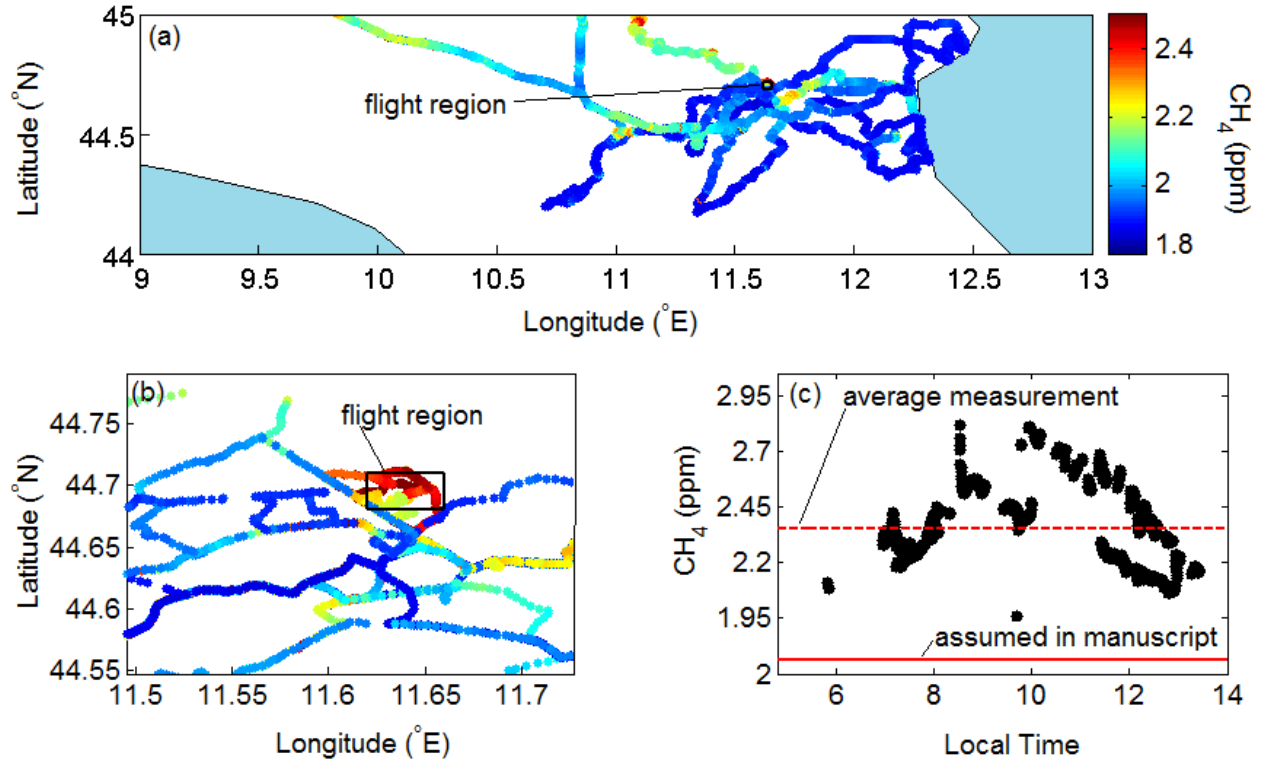


Figure R1. (a) Po-Valley methane measurements acquired from the MOSQUITA during PEGASOS 2012 (b) Zoomed in region highlighting the enhanced methane in the flight region (c) Time series of methane measurements acquired in the boxed region of (b).

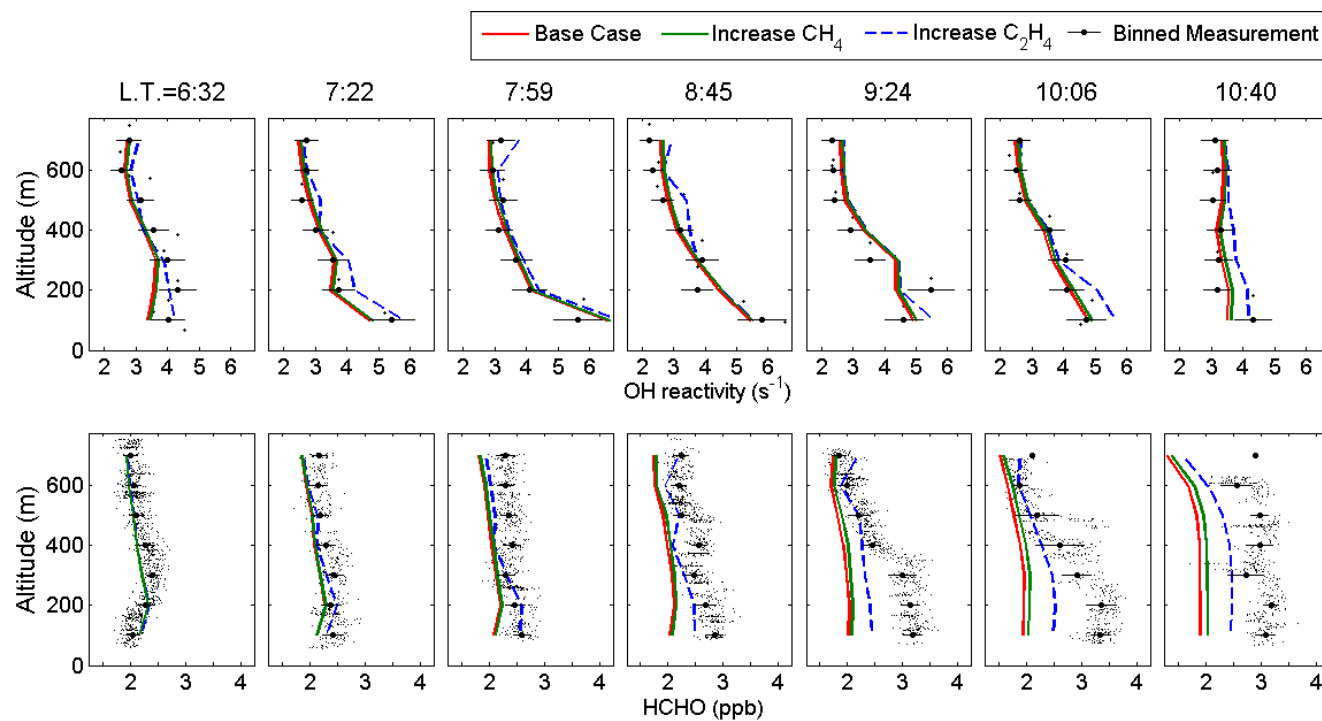


Figure R2. Modeled and measured HCHO and OH reactivity for the base case and increased ethene scenarios as described in the manuscript and shown in Figure 3. The increased CH_4 scenario represents the base case scenario altered such that the average of the MOSQUITA measurements (2355 ppb) is used rather than the global background (1760 ppb).

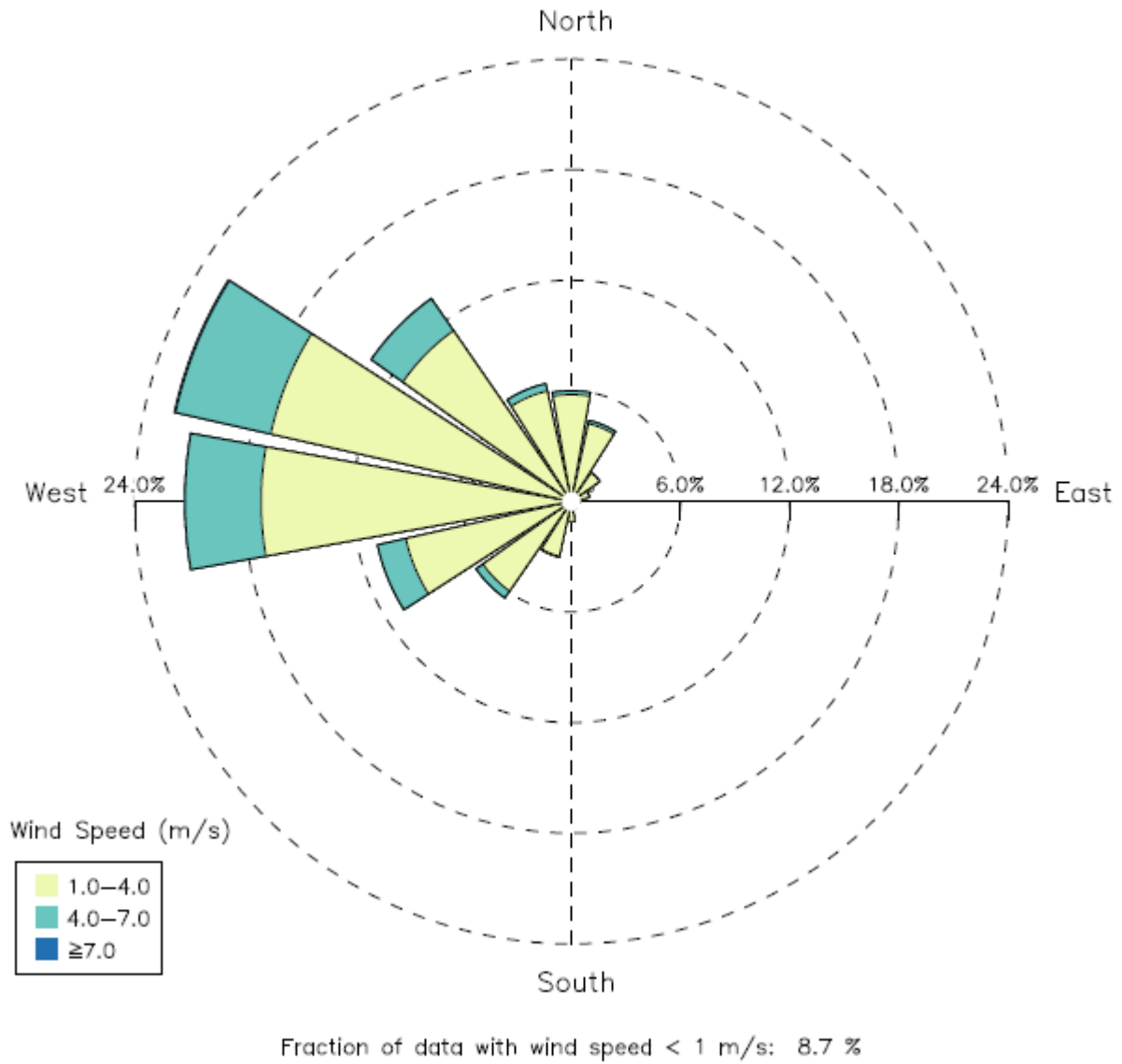


Figure R3. Wind measurements acquired on the July 12th flight.

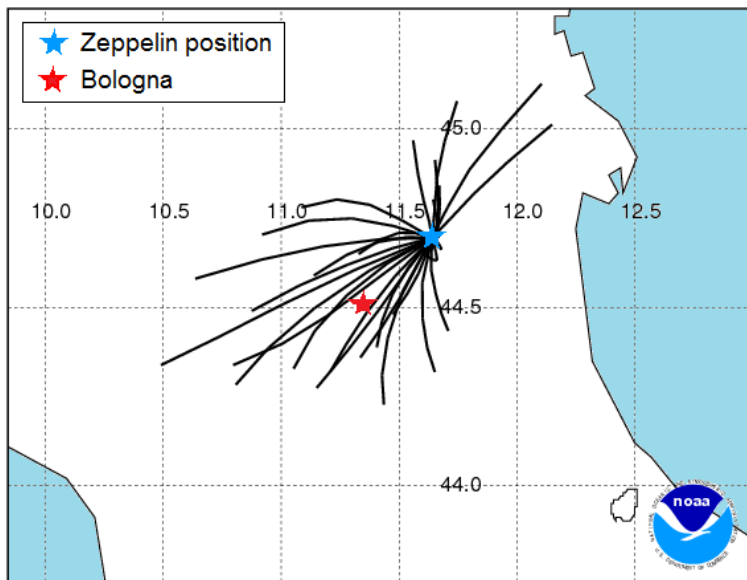


Figure R4. 4 hour HYSPLIT backtrajectories ending at the Zeppelin's position at the time of the observed increase in HCHO.

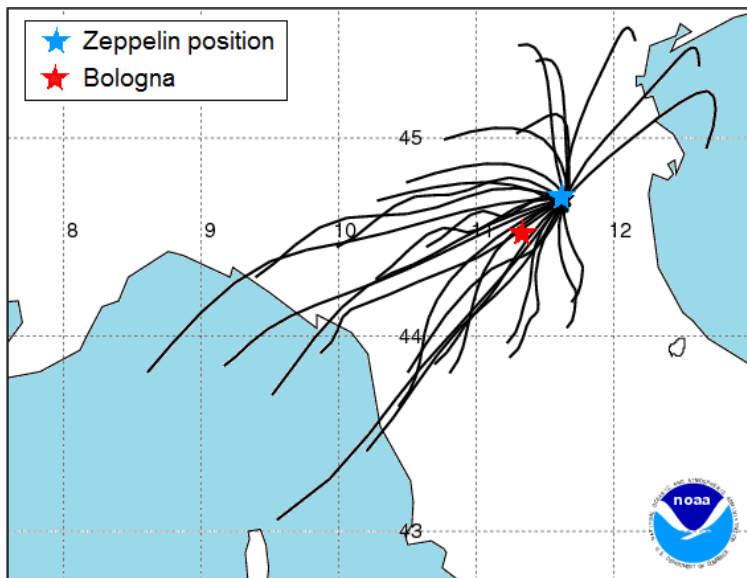


Figure R5. 12 hr HYSPLIT backtrajectories ending at the Zeppelin's position at the time of the observed increase in HCHO.

1 | **Evidence for an unidentified non-photochemical ground-level**
2 | **source of formaldehyde in the Po Valley with potential**
3 | **implications for ozone production**

4
5 | **J. Kaiser¹, G. M. Wolfe^{1*}, B. Bohn², S. Broch², H. Fuchs², L. N. Ganzeveld³, S.**
6 | **Gomm², R. Häsel², A. Hofzumahaus², F. Holland², J. Jäger², X. Li², I. Lohse², K.**
7 | **Lu^{2,**}, A. S. H. Prévôt⁴, F. Rohrer², R. Wegener², R. Wolf⁴, T. F. Mentel², A. Kiendler-**
8 | **Scharr², A. Wahner², and F. N. Keutsch¹**

9 | ¹Chemistry, University of Wisconsin-Madison, Madison, WI

10 | ²Institut für Energie- und Klimaforschung Troposphäre IEK-8, Forschungszentrum Jülich
11 | GmbH, Jülich, Germany

12 | ³Earth System Science and Climate Change, Wageningen University and Research Center,
13 | Wageningen, Netherlands

14 | ⁴Laboratory of Atmospheric Chemistry, Paul Scherrer Institute, Villigen, Switzerland

15 | * now at Joint Center for Earth Systems Technology, University of Maryland Baltimore County,
16 | Baltimore, MD, and at Atmospheric Chemistry and Dynamics Laboratory, NASA Goddard
17 | Space Flight Center, Greenbelt, MD

18 | ** now at College of Environmental Sciences & Engineering, Peking University, Beijing, China

19 | Correspondence to: F. N. Keutsch (keutsch@chem.wisc.edu)

20

21 | **Abstract**

22 | Ozone concentrations in the Po Valley of Northern Italy often exceed international regulations.
23 | As both a source of radicals and an intermediate in the oxidation of most volatile organic
24 | compounds (VOCs), formaldehyde (HCHO) is a useful tracer for the oxidative processing of
25 | hydrocarbons that leads to ozone production. We investigate the sources of HCHO in the Po
26 | Valley using vertical profile measurements acquired from the airship Zeppelin NT over an

1 agricultural region during the PEGASOS 2012 campaign. Using a 1-D model, the total VOC
2 oxidation rate is examined and discussed in the context of formaldehyde and ozone production in
3 the early morning. While model and measurement discrepancies in OH reactivity are small (on
4 average $3.4\% \pm \text{+13}\%$), HCHO concentrations are underestimated by as much as 1.5 ppb (45%)
5 in the convective mixed layer. A similar underestimate in HCHO was seen in the 2002-2003
6 FORMAT Po-Valley measurements, though the additional source of HCHO was not identified.
7 Oxidation of unmeasured VOC precursors cannot explain the missing HCHO source, as
8 measured OH reactivity is explained by measured VOCs and their calculated oxidation products.
9 We conclude that local direct emissions from agricultural land are the most likely source of
10 missing HCHO. Model calculations demonstrate that radicals from degradation of this non-
11 photochemical HCHO source increase model ozone production rates by as much as 0.76 ppb/hr
12 ($\text{+12}\%$) before noon.

13

14 **1 Introduction**

15 Stagnant air masses, abundant solar radiation, and high anthropogenic emissions make Northern
16 Italy's Po Valley one of Europe's most polluted regions. Previous measurements have shown
17 that the regional O₃ background can reach as high as 90 ppb (Liu et al., 2007). Photochemical
18 ozone production is tied to the reactions of NO_x (NO+NO₂), HO_x (OH+HO₂), and volatile
19 organic compounds (VOCs). In the troposphere, NO₂ photodissociates to form oxygen atoms
20 (R1), which then react with molecular oxygen to generate O₃ (R2). The partitioning of NO_x
21 between NO and NO₂ determines the production rate of O₃. The hydroxyl-radical (OH) initiated
22 oxidation of VOCs creates peroxy radicals (XO₂ = HO₂ + RO₂) (R3). These radicals shift the
23 partitioning of NO_x radicals towards NO₂ (R4), thus increasing the net ozone production rate.



28 In this analysis, we define the net ozone production rate (P(O₃)) as the calculated difference
29 between the NO₂ photolysis rate (R1) and the rate of NO to NO₂ conversion by O₃.

1 While measuring all VOCs and their oxidation products is non-trivial, formaldehyde (HCHO) is
2 formed in the oxidation of nearly every VOC and thus provides a downstream constraint on this
3 chemistry. In addition, photolysis of HCHO constitutes an important source of HO₂ radicals
4 without consuming OH, effectively accelerating O₃ production via (R4) followed by (R1) and
5 (R2).

6 In 2002-2003, the FORMAT (FORMaldehyde as A Tracer of oxidation in the troposphere)
7 campaign aimed to use HCHO to trace the effect of VOC oxidation on ozone production in the
8 Po Valley. Though modeling efforts focused primarily on the Milan urban plume, an agricultural
9 region upwind of the city was also investigated in the 2003 FORMAT study (Liu et al., 2007).
10 There, HCHO mixing ratios were up to two times higher than those predicted by regional
11 chemistry transport models. Primary emissions were estimated to be a minor source of HCHO in
12 the agricultural region (~10%), and OH-initiated oxidation of underrepresented local biogenic or
13 anthropogenic VOC emissions was cited as the likely cause of underpredicted HCHO. Because
14 the morning increase in HCHO was not well represented, and because the regional background
15 was not well understood, the effect of anthropogenic emissions on the diurnal cycle under
16 polluted conditions could not be reproduced by the model (Junkermann, 2009).

17 While HCHO measurements provide a product-based view of VOC oxidation, direct
18 measurements of OH reactivity, the inverse lifetime of OH, can provide further insight into the
19 instantaneous VOC oxidation rate. OH reactivity is calculated as

20
$$OH \text{ reactivity } (s^{-1}) = \sum_i k_{X_i+OH} [X_i] \quad (1)$$

21 where k_{X_i+OH} are the rate coefficients for the reaction of all species X with OH. Field
22 measurements of OH reactivity have been available since 2001, and Edwards et al. (2013) and
23 Lou et al. (2010) provide summaries of recent comparisons of modeled and measured reactivity
24 in a variety of environments. Notably, measurements in Paris demonstrated that more than half
25 of the measured reactivity in highly aged continental air masses could not be explained by
26 available measurements (Dolgorouky et al., 2012). The authors concluded the missing OH sink
27 was likely (multi)oxidized compounds from processed anthropogenic emissions. Previous work
28 has examined the effect of discrepancies between modeled and measured OH reactivity on
29 calculated O₃ production potentials (Sadanaga et al., 2005; Yoshino et al., 2012). In one study in

1 Tokyo, including unmeasured VOC precursors indicated by OH reactivity measurements
2 increased the calculated ozone production potential by as much as 8 ppb/hr (55%) (Yoshino et
3 al., 2012).

4 Measurements of OH reactivity provide an upper bound on total VOC oxidation, and in
5 conjunction with measurements of OH concentration, the total RO₂ production rate. Similarly, as
6 HCHO is a major source of HO₂, measurements of HCHO place a lower bound on calculated
7 HO₂ production rates. Correcting for any missing OH reactivity or missing HCHO can increase
8 model XO₂ production rates, in turn increasing P(O₃).

9 Here, we provide an analysis of HCHO, OH reactivity, and O₃ production using an extensive set
10 of measurements acquired onboard a Zeppelin airship during the Pan-European Gas-AeroSOIs
11 Climate Interaction Study (PEGASOS) in the Po-Valley region. Through the Zeppelin's slow
12 flight speed, highly spatially and temporally resolved trace gas measurements were acquired (Li
13 et al., 2014). The Zeppelin's unique flight abilities enabled vertical profiling flight tracks from as
14 low as 50 m up to an altitude of ~750 m, making possible assessment of the role of exchange
15 between the nocturnal boundary layer, residual layer, and growing mixed layer. In this study we
16 focus the analysis on one flight for which a clear delineation between those layers occurred (Li et
17 al., 2014). Using a 1-D chemical transport model, we examine the structure and chemical
18 evolution of HCHO vertical profiles. By combining measurements of OH reactivity and VOC
19 precursors, we investigate sources of HCHO in the agricultural regions of the Po-Valley. Finally,
20 we discuss the effects of HCHO sources on calculated ozone production rates as a function of
21 time and altitude.

22

23 **2 Methods**

24 **2.1 Zeppelin NT payload and July 12th flight**

25 The Zeppelin NT platform, its scientific payload, and the July 12th flight have been described
26 previously (Li et al., 2014) and are described briefly here. Between 05:30 L.T. (Local Time =
27 UTC + 2 h) and 10:45 L.T., the airship performed a series of near-surface vertical spirals starting
28 at 50 m and reaching ~750 m above sea level (Fig. 1). The airship spiraled upward for ~15 min
29 and then returned to lower altitudes within 5 min. The spirals were performed near a ground-

1 based field site at San Pietro Capofiume (SPC, 44°41'N, 11°38'E), which is a background urban
2 site according to the European Monitoring and Evaluation Programme (EMEP) criteria
3 (<http://www.nilu.no/projects/ccc/manual/>). The nearest urban areas include Bologna 25 km to the
4 southwest and Ferrara 20 km to the north. The more immediate region consists primarily of
5 wheat and corn fields which experienced intense harvesting activities during the campaign.

6 The instrumentation, time resolution, accuracy, and precision of the measurements are fully
7 described in Li et al. (2014) and are summarized here (Table 1). Specifically, HCHO was
8 measured at the Zeppelin nose boom using Fiber Laser-Induced Fluorescence (FILIF) (Hottle et
9 al., 2009; DiGangi et al., 2011; Kaiser et al., 2014). The time resolution, precision, and accuracy
10 of the measurement are 1 s, 20 – 200 ppt, and 15%, respectively. The 2 σ detection limit is 40 ppt.
11 OH reactivity was measured from a platform on top of the Zeppelin by flash photolysis of ozone
12 combined with time resolved OH detection in a flow tube. The instrument is an improved, more
13 compact version of the instrument described by Lou et al. (2010). The accuracy of the OH
14 reactivity data is 10%, with $\pm 0.5 \text{ s}^{-1}$ systematic error of the zero-air decay rate coefficients
15 (Gomm, 2014). Speciated C4-C11 VOCs, acetonitrile, and select oxygenated VOCs were
16 measured by a fast gas chromatograph / mass spectrometer system with a time resolution of 180
17 s and 1 σ precision between 3% and 10% (Jäger, 2014). In addition, OH, HO₂, NO, NO₂, O₃,
18 CO, HONO, particle concentration/size distribution, solar actinic flux densities, temperature,
19 pressure, relative humidity, and 3-D wind were measured simultaneously.

20 **2.2 Model simulations**

21 The Chemistry of Atmosphere-Forest Exchange (CAFE) model is a 1-D chemical transport
22 model which has previously been used in steady-state analysis of trace gas fluxes above a pine
23 forest (Wolfe and Thornton, 2011; Wolfe et al., 2011). For this study, the CAFE framework has
24 been adapted to run in a time-dependent manner, and as the region is not forested, no canopy
25 structure is included. The chemical mechanism generated by the Master Chemical Mechanism
26 (MCM) v3.2 ([Jenkin et al., 1997](#); Saunders et al., 2003; [JenkinBloss et al., 19972005](#)) contains
27 near-explicit degradation schemes for all constrained VOCs as well as all relevant inorganic
28 chemistry. (more information available at <http://mcm.leeds.ac.uk/MCM>). The model was run
29 with 7 evenly spaced altitude bins, with altitudes from 50-150 m for the lowest box and 650-750
30 m for the highest box. Measurements acquired during Zeppelin ascents were averaged into these

1 | 100 m altitude bins. Because descents were performed much more quickly than ascents, data
2 | acquired during the ascents have higher spatial resolution than descent data. Where instrument
3 | time resolution limits data availability, concentrations are interpolated from data at surrounding
4 | altitude and time bins. In all model scenarios, measured photolysis frequencies are used where
5 | available. Otherwise, MCM calculated values are scaled according to the ratio of the calculated
6 | and measured photolysis rate of NO₂.

7 | While methane was not measured at the SPC groundsite or from the Zeppelin, measurements of
8 | CH₄ were acquired from a mobile aerosol and trace gas laboratory ("Measurements Of Spatial
9 | QUantitative Immissions of Trace gases and Aerosols": MOSQUITA; Bukowiecki et al., 2002;
10 | Mohr et al., 2011), which was equipped with a Picarro Cavity Ring-Down Spectroscopy analyzer
11 | (Model G2401). MOSQUITA-based CH₄ measurements were acquired from 8 June 2012 to 9
12 | July 2012. Though measurements are not available for the day of the flight studied here, the
13 | average concentration in the flight region of the Zeppelin (2355 ppb) is applied to this study.

14 | In the base case scenario, the model is constrained to all measurements with the exception of
15 | HCHO. Given the extensive constraints, deposition, emission, and advection are not treated
16 | explicitly. Because deposition can be a non-negligible sink for many oxidized species (including
17 | HCHO), model results represent an upper limit on calculated mixing ratios. Turbulent diffusion
18 | is represented using K-theory, where diffusion coefficients are calculated using the Single
19 | Column chemistry and climate Model ECHAM4(SCM) (Ganzeveld et al., 2002). Further
20 | discussion of the eddy diffusion coefficient, uncertainty associated with turbulent diffusion, and
21 | the potential influence of deposition is available in the supplemental information.

22 | To initialize non-measured species (e.g. speciated RO₂ and organic nitrates), a "spin-up" 0-D
23 | diurnal model run was performed constraining all species to a combination of the lowest altitude
24 | Zeppelin measurements and available measurements from the nearby SPC ground site acquired
25 | between June 12th to July 10th 2012. This includes average diurnal profiles of CO, O₃, benzene,
26 | toluene, NO_x, and relevant meteorological parameters. ~~The global background of 1760 ppb~~
27 | ~~methane~~An average methane concentration of 2355 ppb from the MOSQUITA mobile laboratory
28 | was assumed. Anthropogenic VOCs were scaled to ground benzene measurements according
29 | their observed relationship with benzene measurements acquired on the Zeppelin. To mimic the
30 | temperature dependence of isoprene emission rates, isoprene mixing ratios were assumed to be

1 proportional to the cosine of the solar zenith angle and scaled to available Zeppelin
2 measurements. As isoprene concentrations are small (< 100 ppt), the diurnal cycle has a
3 negligible impact on modeled results. For 1-D model simulations, non-measured species are
4 initialized to the output of the spin-up model at 06:00 L.T. on the 4th day scaled to HCHO
5 measured on the Zeppelin as a function of altitude.

6

7 **3 Results and Discussion**

8 **3.1 Observed HCHO and OH reactivity**

9 In the following section, we present observations of HCHO, VOCs, and OH reactivity acquired
10 on the July 12th flight in the context of previous Po Valley measurements. A detailed
11 presentation of additional trace gas measurements (notably HONO, NO_x, O₃, HO₂, and H₂O) as
12 well as discussion of the delineation between residual layer, nocturnal boundary layer, and mixed
13 layer can be found in Li et al. (2014).

14 Figure 2 shows measured HCHO, OH reactivity, and selected VOCs as a function of time and
15 altitude. Primary biogenic VOC concentrations were low throughout the entire flight (isoprene $<$
16 60 ppt), which is consistent with previous measurements at Verzago, an agriculture site
17 downwind of Milan (Steinbacher et al., 2005a). Anthropogenic VOCs such as toluene and
18 benzene were around an order of magnitude lower than at Verzago in 2003 (Steinbacher et al.,
19 2005b). In contrast to primary biogenic and anthropogenic VOCs, oxidized VOCs were abundant
20 (reaching HCHO > 3.8 ppb, acetaldehyde > 1.0 ppb). The overall magnitude and morning rise of
21 HCHO observed were similar to those observed previously in Spessa in 2002 (Junkermann,
22 2009).

23 Before sunrise, elevated levels of toluene and other anthropogenic VOCs were observed in the
24 residual layer compared to lower altitudes. Accumulation of VOC oxidation products including
25 HCHO, methacrolein, and acetaldehyde was observed in the nocturnal boundary and in the
26 residual layer. These oxidation products are either built up overnight or remain elevated from the
27 previous day. After sunrise (05:45 L.T.), both biogenic and anthropogenic primary VOC increase
28 in the developing mixed layer. The observed increase in HCHO mixing ratios lags that of
29 primary VOCs, so that higher HCHO concentrations were observed ~ 4 hrs after sunrise. The

1 general vertical structure of the observed OH reactivity tracks well with HCHO, with elevated
2 values in nocturnal boundary and growing mixed layers. Based on the vertical structure of the
3 observed HCHO and other trace gasses, potential sources of HCHO are discussed further in
4 section 3.3.

5 **3.2 Base scenario modelled OH reactivity and HCHO**

6 The top panel of Fig. 3 shows the measured and modeled OH reactivity as a function of time and
7 altitude. Overall, the magnitude and vertical structure is well captured by measured VOCs and
8 their oxidation products. Where underestimated, the average discrepancy is less than ~~40~~7%, with
9 larger discrepancies at lower altitudes. Speciated model contributions to OH reactivity are shown
10 in Fig. 4, calculated with all species (including HCHO) constrained to observations. NO_x
11 strongly influences the modeled OH reactivity ~~was dominated by NO_x and CO, with VOCs,~~
12 contributing ~~more~~40% to modeled reactivity at 100 m, 8:45 L.T. The contribution of measured
13 VOCs and OVOCs is most significant in the mixed layer. ~~Of all VOCs, (26% at 100 m, 8:45~~
14 L.T.). Of all VOCs and OVOCs, HCHO consistently contributes the largest portion of calculated
15 OH reactivity (HCHO reactivity ~ 0.2 s⁻¹ ppb⁻¹), 8% of total modeled reactivity at 100 m and
16 8:45 L.T.).

17 Figure 3 also shows measured and modeled HCHO. Before 09:00 L.T., base case modeled
18 HCHO matches measurements quite well. This is expected, as the model is initialized to
19 measured HCHO mixing ratios, and low OH concentrations as well as lack of photolysis lead to
20 very little change. Model/measurement discrepancy grows with time and is largest at low
21 altitudes. Between 06:32 L.T. and 10:06 L.T., HCHO increases by as much as 1.3 ppb, while the
22 model predicts no net increase. HCHO loss terms are unlikely to be overestimated as they are
23 constrained by measured OH and measured HCHO photolysis frequencies, and could potentially
24 be underestimated by neglecting deposition (see supplement). This finding implies that the
25 model is missing either chemical HCHO production, advection of HCHO, or a local source of
26 direct HCHO emissions.

27 **3.3 Potential sources of HCHO**

28 The oxidation of additional non-measured VOCs is often cited as a possible source of missing
29 HCHO production in models (~~compare~~compared to FORMAT study, Junkermann, 2009). Using

1 OH reactivity measurements, one can place an upper bound on the overall VOC oxidation rate in
2 the atmosphere. As discussed above, measured VOCs and their modeled oxidation products
3 explain the majority of observed OH reactivity, though a small discrepancy is occasionally
4 observed. To investigate the possibility of non-measured HCHO precursors, an additional model
5 scenario is constructed in which the missing OH reactivity is assumed to be comprised entirely
6 of ethene (C₂H₄). C₂H₄ was chosen as a surrogate species because it produces HCHO from OH
7 and O₃ oxidation with respective yields of 160% (Niki et al., 1981) and 154% (Alam et al.,
8 2011). Thus, the increase in modeled HCHO per increase in calculated OH reactivity is
9 maximized.

10 Figure 3 shows the effect of increasing C₂H₄ on HCHO and OH reactivity. While measured
11 mixed-layer HCHO increases by as much as 1.3 ppb between 6:30 and 10:00 L.T., model HCHO
12 increases by only ~~330~~300 ppt. In order to generate the required HCHO, modeled C₂H₄ would
13 need to be increased such that calculated OH reactivity is up to ~~455~~6% greater than the
14 measurements. While the model vertical profile at 10:40 L.T. is in better agreement with
15 measurements, at the 09:24 L.T. vertical profile additional VOC precursors can explain no more
16 than 0.~~422~~6 ppb, or ~~332~~3%, of the missing HCHO budget. We therefore conclude that non-
17 measured VOCs cannot explain the discrepancy in measured and modeled HCHO.

18 Another possible source of HCHO is transport from nearby urban centers. In the early morning,
19 the average wind speed was less than 1.2 m/s, and the average HCHO lifetime was ~3.5 hr.
20 Between 6:00 L.T. and 10:30 L.T., the bottom most layer in contact with the surface grows from
21 less than 50 m to more than 600 m in height. Accounting for this dilution, and the HCHO
22 lifetime and wind speed, and assuming a nighttime concentration in Bologna of 6 ppb (near the
23 maximum nocturnal concentration reported in Milan (Junkermann, 2009)), the amount of HCHO
24 advected could be no more than 90 ppt, or 7% of the missing HCHO budget. Additionally, no
25 other long-lived tracers of anthropogenic influence (i.e. CO, xylenes) show a rise in the late
26 morning. Finally, the vertical profile of the missing HCHO suggests a strong source near the
27 ground which is convectively incorporated into the growing mixed layer. As advection of
28 HCHO, e.g., from Bologna, would more likely affect the mixed layer as a whole, transport is an
29 unlikely source of HCHO.

1 As the air aloft initially has slightly elevated levels of HCHO, entrainment of air from the
2 residual layer into the mixed layer is an additional potential source of HCHO. Using
3 ECHAM4(SCM) to investigate observations from the October 2005 field campaign over the
4 Atlantic Ocean, French Guyana and Suriname, Ganzeveld et al. (2008) demonstrated the
5 assessment of daytime HCHO requires a thorough evaluation of the morning turbulent transport.
6 The model predicted entrainment of HCHO would affect the daytime radical budget and
7 resulting oxidative chemistry; however, limited observations in the residual layer did not allow
8 for comparing SCM simulations with measurements. If entrainment was the primary cause of
9 measurement and model discrepancy, the missing HCHO would be larger near the top of the
10 boundary layer and when HCHO concentrations aloft are the highest. In this study, the largest
11 discrepancies occur at the lowest altitudes and later in the morning. The highly resolved vertical
12 measurements enabled by the Zeppelin aircraft demonstrate that for this study, entrainment is
13 unlikely to be the primary cause of model/measurement discrepancies at low altitudes.

14 An additional potential source of HCHO is local direct emission from biomass burning or other
15 anthropogenic activities. Aircraft measurements in 2003 showed evidence of biomass burning
16 contribution to elevated HCHO in the agricultural regions of the Po Valley (Junkermann, 2009);
17 however, these measurements were in September and October after the harvesting of the rice
18 fields, and we did not see such strong local sources during the flight. Acetonitrile, a tracer of
19 biomass burning, remains at a background levels of < 250 ppt. As CO is a product of incomplete
20 fuel combustion, it can be used to trace the influence of local traffic. CO does not increase
21 significantly during the time HCHO increases in the mixed layer (Fig. 5). Using an emission
22 ratio of 3.14 g HCHO/kg CO observed at a highway junction in Houston, Texas (Rappenglueck
23 et al., 2013), the increase of 19 ppb in CO between 06:20 and 10:00 L.T., if wholly from traffic
24 emissions, could account for only 57 ppt (4%) of the observed increase in HCHO. We therefore
25 conclude neither biomass burning nor traffic can account for the relatively high levels of
26 observed HCHO.

27 Finally, the soil, decaying plant matter from harvesting, or wheat or other crops in the region of
28 the Zeppelin spirals may be a source of local direct HCHO emission. Measurements of
29 oxygenated VOCs (OVOCs) from agricultural crops are limited. Konig et al. (1995) reported
30 total OVOC emission rates from wheat were of $10.9 \text{ ng g}^{-1} \text{ h}^{-1}$, though speciated measurements
31 of formaldehyde were not available. Dry weight HCHO emission rates from tree species in Italy

1 are much higher, ranging from 382 to 590 ng g⁻¹h⁻¹ (Kesselmeier et al., 1997). Oxygenated VOC
2 emissions are expected to respond differently to light and temperature than terpenoids (Rinne et
3 al., 2007), nevertheless the classic terpenoid exponential model is often extended to OVOC
4 emissions. For example, for ground emissions of HCHO in a ponderosa pine forest, DiGangi et
5 al. (2011) applied an emission algorithm of $E_{\text{HCHO}}=A \cdot \exp(\beta T)$, where $A=740 \text{ ng m}^{-2} \text{ h}^{-1}$ and $\beta =$
6 $0.07 \text{ }^\circ\text{C}^{-1}$. The emissions were scaled by photosynthetically active radiation, with night time
7 emissions fixed to 15% of daytime.

8 A final model scenario was constructed which incorporates direct emissions of HCHO according
9 to the sunlight-weighted exponential emission function similar to DiGangi et al., employing a
10 much smaller prefactor of $A=375 \text{ ng m}^{-2} \text{ h}^{-1}$ to best capture the observed HCHO mixing ratios.
11 These emissions are added as a direct HCHO source for the model's surface layer (0-50 m), with
12 all other surface layer concentrations constrained to their lowest altitude measurement. The
13 results are shown in Fig. 3. The vertical profile is mostly consistent with measurements, with
14 possible discrepancies arising from uncertainty in eddy diffusion constants (see supplement).
15 Due to the good agreement of this model result and the improbability of other HCHO sources,
16 we conclude local direct emissions from agricultural land are the most likely source of additional
17 HCHO.

18 The finding that direct biogenic emission could account for a large percentage of the observed
19 increase in HCHO mixing ratio is in contrast with the Liu et al. (2007) assumption that direct
20 emissions accounts for only ~10% of HCHO source in the agricultural Po Valley. Due to scarce
21 data availability, limited information on chemical speciation, and only rough estimation of
22 emission rates, models often assume a default emission rate for all oxygenated VOCs
23 independent of land use or plant type (Karl et al., 2009). To realize the full potential of these
24 oxidized VOCs as tracers of the photochemistry that forms secondary pollutants, and to
25 understand their effects on such chemistry, thorough studies of direct emission are needed.

26 **3.4 Implications for ozone production**

27 An additional HCHO source, regardless of the type, will have a direct impact on calculated
28 ozone production rates. The in-situ ozone production can be calculated as

$$29 \quad P(O_3) = k_{HO_2+NO}[HO_2][NO] + \sum_i k_{RO_2+NO}[RO_2][NO], \quad (2)$$

1 where NO₂ is assumed to photodissociate leading to immediate ozone production (R1 and R2).
2 In our MCM-based calculations, the formation of ~~organonitrates~~ organic nitrates is accounted for
3 in the RO₂ + NO reaction rates. As direct measurements of RO₂ were not available on the
4 Zeppelin, the analysis presented here relies on speciated modeled RO₂ concentrations and
5 reaction rates. Typical model RO₂ concentrations are between 10% and 30% of the sum of
6 modeled RO₂ and measured HO₂, such that HO₂ accounts for the majority of the modeled NO to
7 NO₂ conversion. Because HCHO photolysis and oxidation accounts for as much as 4539%
8 model HO₂ production, failing to include all sources of HCHO has significant effects on
9 calculated HO₂ concentrations. Though not probable in this analysis, if oxidation of unmeasured
10 VOCs contributes significantly to the HCHO budget, RO₂ concentrations would likely be
11 underestimated.

12 ~~Because measured HO₂ had large uncertainty and because~~ Because the effects of transport on O₃
13 may be large, we do not explicitly compare measured and modeled ~~HO₂ or O₃~~ concentrations in
14 this study. Instead, two model scenarios were constructed to estimate the impact of missing
15 HCHO on HO₂ mixing ratios and therefore ozone production. Both simulations were carried out
16 with HO₂ unconstrained, and HCHO was either fixed to observations or calculated by the model.

17 ~~While both model runs produced~~ Constraining HO₂ has a negligible effect on modeled HCHO
18 ~~concentrations within the uncertainty of measurements, differences.~~ Because the difference in
19 concentration of HO₂ mixing ratios in ~~between~~ the two model scenarios ~~were observed (up~~
20 smaller than the measurement uncertainty (~12% compared to 2 ppt)-30%), and because both
21 model scenarios reproduce HO₂ concentration within the measurement uncertainty, measured
22 and modeled HO₂ are not compared. At the observed mixed layer NO concentrations of ~1 ppb
23 and an rate constant of $k_{\text{HO}_2+\text{NO}} = 8.6 \cdot 10^{-12} \text{ cm}^3 \text{ molec}^{-1} \text{ s}^{-1}$, an increase of just 1 ppt HO₂
24 corresponds to an additional 0.7 ppb/hr (4014%) of ozone production. Figure 6 shows the
25 difference in P(O₃) driven by differences in calculated HO₂ concentrations. Assuming the trend
26 in the discrepancy in HCHO continues to increase throughout the day, an increasing under-
27 prediction of local ozone production rate is expected for this agricultural region.

28

1 **4 Conclusions**

2 Using a near-explicit 1-D model and a comprehensive set of trace gas measurements acquired
3 from a Zeppelin airship, we have examined VOC oxidation and its relationship to ozone
4 production in the Po Valley. As in previous work in the region, our model was largely unable to
5 reproduce the morning rise and high levels of observed HCHO. Measured OH reactivity,
6 however, was explained by measured VOCs and their calculated oxidation products. The most
7 probable source of missing HCHO is direct emission from the soil and plant matter beneath the
8 Zeppelin. As a result of the underestimate in HCHO, model ozone production rates based on
9 HO₂ concentrations are underestimated by as much as ~~+0~~+12% before noon, and the underestimate
10 is expected to increase. When considering photochemical models of O₃ production, even small
11 underestimates in HCHO can lead to large underestimates of local ozone production rates. For
12 that reason, and considering the large portion of land used globally for similar agricultural
13 purposes, direct measurements of OH reactivity and HCHO as well as improved OVOC emission
14 inventories would aid in the prediction of high ozone events.

15

16 **Acknowledgements**

17 This work is within the PEGASOS project which is funded by the European Commission under
18 the Framework Programme 7 (FP7-ENV-2010-265148). The authors would like to acknowledge
19 all members of the PEGASOS flight and science teams. We also acknowledge Zeppelin
20 Luftschifftechnik (ZLT) and Deutsche Zeppelin Reederei (DZR) for their cooperation. J. Jäger,
21 R. Wegener, I. Lohse, and B. Bohn like to thank Deutsche Forschungsgemeinschaft for funding
22 within the priority program HALO (WE-4384/2-2 and BO1580/4-1). J. Kaiser, G. M. Wolfe, and
23 F. Keutsch like to thank Maria Cazorla for helping with the calibration of the HCHO
24 measurements and NSF-AGS (1051338) and Forschungszentrum Jülich for support. G. Wolfe
25 acknowledges support from the NOAA Climate and Global Change Postdoctoral Fellowship
26 Program. J. Kaiser acknowledges support from the National Science Foundation Graduate
27 Research Fellowship Program under Grant No. DGE-1256259. We would like to thank ARPA
28 Emilia-Romagna (Region Agency for Environmental Protection in the Emilia-Romagna region
29 Italy) and all participants in the Supersito Project for providing measurements at the SPC
30 groundsite. The authors also acknowledge Christos Kaltsonoudis and Spyros Pandis from

1 Laboratory of Air Quality Studies at the University of Patras for making CO data from the SPC
2 ground site available.

3

4 **References**

5 Alam, M. S., Camredon, M., Rickard, A. R., Carr, T., Wyche, K. P., Hornsby, K. E., Monks, P.
6 S., and Bloss, W. J.: Total radical yields from tropospheric ethene ozonolysis, *Phys. Chem.*
7 *Chem. Phys.*, 13, 11002-11015, 10.1039/c0cp02342f, 2011.

8 [Bloss, C., Wagner, V., Jenkin, M. E., Volkamer, R., Bloss, W. J., Lee, J. D., Heard, D. E., Wirtz,](#)
9 [K., Martin-Reviejo, M., Rea, G., Wenger, J. C., and Pilling, M. J.: Development of a detailed](#)
10 [chemical mechanism \(MCMv3.1\) for the atmospheric oxidation of aromatic hydrocarbons,](#)
11 [Atmos. Chem. Phys., 5, 641-664, doi:10.5194/acp-5-641-2005, 2005.](#)

12 Bohn, B., Corlett, G. K., Gillmann, M., Sanghavi, S., Stange, G., Tensing, E., Vrekoussis, M.,
13 Bloss, W. J., Clapp, L. J., Kortner, M., Dorn, H.-P., Monks, P. S., Platt, U., Plass-Dülmer, C., Mi-
14 halopoulos, N., Heard, D. E., Clemitshaw, K. C., Meixner, F. X., Prevot, A. S. H., and Schmitt,
15 R.: Photolysis frequency measurement techniques: results of a comparison within the ACCENT
16 project, *Atmos. Chem. Phys.*, 8, 5373–5391, doi:10.5194/acp-8- 5373-2008, 2008.

17 [Bukowiecki, N., Dommen, J., Prévôt, A. S. H., Richter, R., Weingartner, E., and Baltensperger,](#)
18 [U.: A mobile pollutant measurement laboratory – measuring gas phase and aerosol ambient](#)
19 [concentrations with high spatial and temporal resolution. Atmos. Environ., 36, 5569–5579, doi:](#)
20 [10.1016/S1352-2310\(02\)00694-5, 2002.](#)

21 DiGangi, J., Boyle, E., Karl, T., Harley, P., Turnipseed, A., Kim, S., Cantrell, C., Maudlin, R.,
22 Zheng, W., Flocke, F., Hall, S., Ullmann, K., Nakashima, Y., Paul, J., Wolfe, G., Desai, A.,
23 Kajii, Y., Guenther, A., and Keutsch, F.: First direct measurements of formaldehyde flux via
24 eddy covariance: implications for missing in-canopy formaldehyde sources, *Atmos. Chem.*
25 *Phys.*, 11, 10565-10578, 10.5194/acp-11-10565-2011, 2011.

26 Dolgorouky, C., Gros, V., Sarda-Estève, R., Sinha, V., Williams, J., Marchand, N., Sauvage, S.,
27 Poulain, L., Sciare, J., and Bonsang, B.: Total OH reactivity measurements in Paris during the
28 2010 MEGAPOLI winter campaign, *Atmos. Chem. Phys.*, 12, 9593-9612, 10.5194/acp-12-9593-
29 2012, 2012.

1 Edwards, P., Evans, M., Furneaux, K., Hopkins, J., Ingham, T., Jones, C., Lee, J., Lewis, A.,
2 Moller, S., Stone, D., Whalley, L., and Heard, D.: OH reactivity in a South East Asian tropical
3 rainforest during the Oxidant and Particle Photochemical Processes (OP3) project, *Atmos. Chem.*
4 *Phys.*, 13, 9497-9514, 10.5194/acp-13-9497-2013, 2013.

5 Fuchs, H., Bohn, B., Hofzumahaus, A., Holland, F., Lu, K., Nehr, S., Rohrer, F., and Wahner,
6 A.: Detection of HO₂ by laser-induced fluorescence: calibration and interferences from RO₂
7 radicals, *Atmos. Meas. Techn.*, 4, 1209-1225, 10.5194/amt-4-1209-2011, 2011.

8 Ganzeveld, L., Lelieveld, J., Dentener, F., Krol, M., and Roelofs, G.: Atmosphere-biosphere
9 trace gas exchanges simulated with a single-column model, *J. Geophys. Res.-Atmos.*, 107,
10 10.1029/2001JD000684, 2002.

11 Ganzeveld, L., Eerdeken, G., Feig, G., Fischer, H., Harder, H., Konigstedt, R., Kubistin, D.,
12 Martinez, M., Meixner, F., Scheeren, H., Sinha, V., Taraborrelli, D., Williams, J., de Arellano, J.,
13 and Lelieveld, J.: Surface and boundary layer exchanges of volatile organic compounds, nitrogen
14 oxides and ozone during the GABRIEL campaign, *Atmos. Chem. Phys.*, 8, 6223-6243,
15 10.5194/acp-8-6223-2008, 2008.

16 Gerbig, C., Schmitgen, S., Kley, D., Volz-Thomas, A., Dewey, K., and Haaks, D.: An improved
17 fast-response vacuum-UV resonance fluorescence CO instrument, *J. Geophys. Res.*, 104, 1699–
18 1704, doi:10.1029/1998JD100031, 1999.

19 Gomm, S. : Luftgestützte Messung von HOx-Radikalkonzentrationen mittels Laser-induzierter
20 Fluoreszenz auf einem Zeppelin NT: Untersuchung der atmosphärischen Oxidationsstärke der
21 unteren Troposphäre, Ph. D., Bergische-Universität Wuppertal, 2014.

22 Holland, F., Hofzumahaus, A., Schäfer, R., Kraus, A., and Pätz, H. W.: Measurements of OH
23 and HO₂ radical concentrations and photolysis frequencies during BERLIOZ, *J. Geophys. Res.-*
24 *Atmos.*, 108, 10.1029/2001jd001393, 2003.

25 Hottle, J., Huisman, A., Digangi, J., Kamrath, A., Galloway, M., Coens, K., and Keutsch, F.: A
26 Laser Induced Fluorescence-Based Instrument for In-Situ Measurements of Atmospheric
27 Formaldehyde, *Environ. Sci. Technol.*, 43, 790-795, 10.1021/es801621f, 2009.

1 Jäger, J.: Airborne VOC measurements on board the Zeppelin NT during PEGASOS campaigns
2 in 2012 deploying the improved Fast-GC-MSD System, Ph. D., Forschungszentrum Jülich
3 GmbH, Jülich, Germany, 2014.

4 Jenkin, M., Saunders, S., and Pilling, M.: The tropospheric degradation of volatile organic
5 compounds: A protocol for mechanism development, *Atmos. Environ.*, 31, 81-104,
6 10.1016/S1352-2310(96)00105-7, 1997.

7 Junkermann, W.: On the distribution of formaldehyde in the western Po-Valley, Italy, during
8 FORMAT 2002/2003, *Atmos. Chem. Phys.*, 9, 9187-9196, 2009.

9 Kaiser, J., Li, X., Tillmann, R., Acir, I., Holland, F., Rohrer, F., Wegener, R., and Keutsch, F. N.:
10 Intercomparison of Hantzsch and fiber-laser-induced-fluorescence formaldehyde measurements,
11 *Atmos. Meas. Tech.*, 7, 1571-1580, 10.5194/amt-7-1571-2014, 2014.

12 Karl, M., Guenther, A., Koble, R., Leip, A., and Seufert, G.: A new European plant-specific
13 emission inventory of biogenic volatile organic compounds for use in atmospheric transport
14 models, *Biogeosciences*, 6, 1059-1087, 2009.

15 Kesselmeier, J., Bode, K., Hofmann, U., Müller, H., Schäfer, L., Wolf, A., Ciccioli, P.,
16 Brancaleoni, E., Cecinato, A., Frattoni, M., Foster, P., Ferrari, C., Jacob, V., Fugit, J. L., Dutaur,
17 L., Simon, V., and Torres, L.: Emission of short chained organic acids, aldehydes and
18 monoterpenes from *Quercus ilex* L. and *Pinus pinea* L. in relation to physiological activities,
19 carbon budget and emission algorithms, *Atmos. Environ.*, 31, 119-133, 10.1016/s1352-
20 2310(97)00079-4, 1997.

21 König, G., Brunda, M., Puxbaum, H., Hewitt, C. N., Duckham, S. C., and Rudolph, J.: Relative
22 contribution of oxygenated hydrocarbons to the total biogenic VOC emissions of selected Mid-
23 European agricultural and natural plant-species, *Atmos. Environ.*, 29, 861-874, 10.1016/1352-
24 2310(95)00026-u, 1995.

25 Li, X., Rohrer, F., Hofzumahaus, A., Brauers, T., Häseler, R., Bohn, B., Broch, S., Fuchs, H.,
26 Gomm, S., Holland, F., Jäger, J., Kaiser, J., Keutsch, F. N., Lohse, I., Lu, K., Tillmann, R.,
27 Wegener, R., Wolfe, G. M., Mentel, T. F., Kiendler-Scharr, A., and Wahner, A.: Missing Gas-
28 Phase Source of HONO Inferred from Zeppelin Measurements in the Troposphere, *Science*, 344,
29 292-296, 10.1126/science.1248999, 2014.

1 Liu, L., Andreani-Aksoyoglu, S., Keller, J., Ordonez, C., Junkermann, W., Hak, C., Braathen, G.,
2 Reimann, S., Astorga-Llorens, C., Schultz, M., Prevot, A., and Isaksen, I.: A photochemical
3 modeling study of ozone and formaldehyde generation and budget in the Po basin, *J. Geophys.*
4 *Res.-Atmos.*, 112, 10.1029/2006JD008172, 2007.

5 Lou, S., Holland, F., Rohrer, F., Lu, K., Bohn, B., Brauers, T., Chang, C., Fuchs, H., Häsel, R.,
6 Kita, K., Kondo, Y., Li, X., Shao, M., Zeng, L., Wahner, A., Zhang, Y., Wang, W., and
7 Hofzumahaus, A.: Atmospheric OH reactivities in the Pearl River Delta – China in summer
8 2006: measurement and model results, *Atmos. Chem. Phys.*, 10, 11243–11260, doi:10.5194/acp-
9 10-11243-2010, 2010.

10 [Mohr, C., Richter, R., DeCarlo, P. F., Prévôt, A. S. H., and Baltensperger, U.: Spatial variation](#)
11 [of chemical composition and sources of submicron aerosol in Zurich during wintertime using](#)
12 [mobile aerosol mass spectrometer data, *Atmos. Chem. Phys.*, 11, 7465-7482, doi:10.5194/acp-](#)
13 [11-7465-2011, 2011.](#)

14 Niki, H., Maker, P. D., M., S. C., and Breitenbach, L. P.: An FTIR study of mechanisms for the
15 HO radical initiated oxidation of C₂H₄ in the presence of NO: Detection of glycolaldehyde,
16 *Chem. Phys. Lett.*, 80, 499–503, 1981.

17 Rappenglueck, B., Lubertino, G., Alvarez, S., Golovko, J., Czader, B., and Ackermann, L.:
18 Radical precursors and related species from traffic as observed and modeled at an urban highway
19 junction, *JAPCA J. Air Waste Ma.*, 63, 1270-1286, 10.1080/10962247.2013.822438, 2013.

20 Rinne, J., Taipale, R., Markkanen, T., Ruuskanen, T. M., Hellen, H., Kajos, M. K., Vesala, T.,
21 and Kulmala, M.: Hydrocarbon fluxes above a Scots pine forest canopy: measurements and
22 modeling, *Atmos. Chem. Phys.*, 7, 3361-3372, 2007.

23 Sadanaga, Y., Yoshino, A., Kato, S., and Kajii, Y.: Measurements of OH reactivity and
24 photochemical ozone production in the urban atmosphere, *Environ. Sci. Technol.*, 39, 8847-
25 8852, 10.1021/es049457p, 2005.

26 Saunders, S., Jenkin, M., Derwent, R., and Pilling, M.: Protocol for the development of the
27 Master Chemical Mechanism, MCM v3 (Part A): tropospheric degradation of non-aromatic
28 volatile organic compounds, *Atmos. Chem. Phys.*, 3, 161-180, 2003.

1 Steinbacher, M., Dommen, J., Ordonez, C., Reimann, S., Gruebler, F., Staehelin, J., Andreani-
2 Aksoyoglu, S., and Prevot, A. S. H.: Volatile organic compounds in the Po Basin. part B:
3 Biogenic VOCs, *J. Atmos. Chem.*, 51, 293-315, 10.1007/s10874-005-3577-0, 2005a.

4 Steinbacher, M., Dommen, J., Ordonez, C., Reimann, S., Gruebler, F. C., Staehelin, J., and
5 Prevot, A. S. H.: Volatile organic compounds in the Po Basin. part A: Anthropogenic VOCs, *J.*
6 *Atmos. Chem.*, 51, 271-291, 10.1007/s10874-005-3576-1, 2005b.

7 Wolfe, G., and Thornton, J.: The Chemistry of Atmosphere-Forest Exchange (CAFE) Model -
8 Part 1: Model description and characterization, *Atmos. Chem. Phys.*, 11, 77-101, 10.5194/acp-
9 11-77-2011, 2011.

10 Wolfe, G., Thornton, J., Bouvier-Brown, N., Goldstein, A., Park, J., Mckay, M., Matross, D.,
11 Mao, J., Brune, W., LaFranchi, B., Browne, E., Min, K., Wooldridge, P., Cohen, R., Crouse, J.,
12 Faloon, I., Gilman, J., Kuster, W., de Gouw, J., Huisman, A., and Keutsch, F.: The Chemistry
13 of Atmosphere-Forest Exchange (CAFE) Model - Part 2: Application to BEARPEX-2007
14 observations, *Atmos. Chem. Phys.*, 11, 1269-1294, 10.5194/acp-11-1269-2011, 2011.

15 Yoshino, A., Nakashima, Y., Miyazaki, K., Kato, S., Suthawaree, J., Shimo, N., Matsunaga, S.,
16 Chatani, S., Apel, E., Greenberg, J., Guenther, A., Ueno, H., Sasaki, H., Hoshi, J., Yokota, H.,
17 Ishii, K., and Kajii, Y.: Air quality diagnosis from comprehensive observations of total OH
18 reactivity and reactive trace species in urban central Tokyo, *Atmos. Environ.*, 49, 51-59,
19 | 10.1016/j.atmosenv.2011.12.029, 2012.

1
2
3
4
5
6
7
8
9
10
11

12 Table 1. Zeppelin-based measurements used for the analysis of O₃ and HCHO production

Parameter	Technique	Precision (1 σ)	Accuracy
HCHO	FILIF ^a	20-200ppt/s	15%
HONO	LOPAP ^b	1.3 ppt/180 s	12%
OH	Laser induced fluorescence ^c	Day LOD: 1.3x 10 ⁶ cm ⁻³ /42 s Night LOD: 0.67x 10 ⁶ cm ⁻³ /42 s	14%
HO ₂	Laser induced fluorescence ^d	Day LOD: 81 x 10 ⁶ cm ⁻³ /42 s Night LOD: 36x 10 ⁶ cm ⁻³ /42 s	24-30%
OH reactivity	Laser induced fluorescence ^e	6%/2 min (standarddeviation)	10%
NO	Chemiluminescence ^f	10 ppt/60 s	5%
NO ₂	Conversion to NO ^g followed by chemiluminescence ^f	30 ppt/60 s	7.5%
O ₃	UV absorption ^h	1 ppb/20 s	3%
CO	Resonance fluorescence ⁱ	5 ppb/1 s	5%
VOCs	Fast GC/MS ^j	3-10%/180 s	15%
Photolysis frequencies	Spectroradiometer ^k	-- (1 s) ^k	15% ^k

Relative humidity	Vaisala HUMICAP HMP45	0.1% RH/1 s	2% RH
Temperature	PT100	0.1 °C/1 s	0.1 °C
Pressure	Barometric SETRA	<0.5 mbar/1 s	33 mbar

1 ^aFiber laser-induced fluorescence (Hottle et al., 2009).

2 ^bLong path absorption photometry (Li et al., 2014).

3 ^cHolland et al., (2003).

4 ^dFuchs et al., (2011).

5 ^eLou et al., (2010).

6 ^fECOPHYSICS (type TR780)

7 ^gPhotolytic blue light converter (Droplet Technologies type BLC)

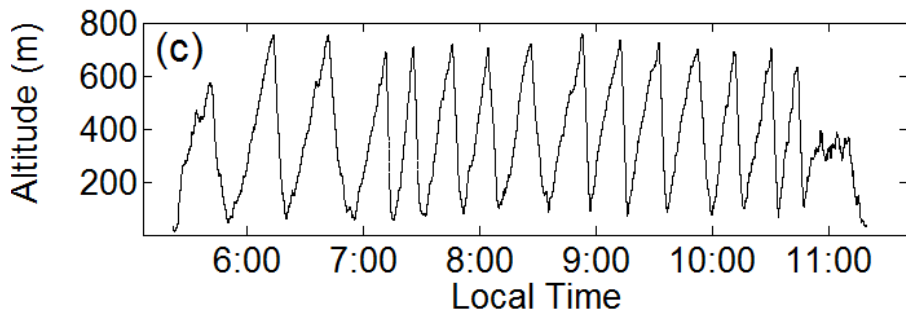
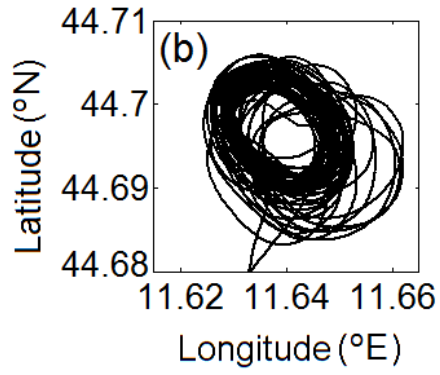
8 ^hENVIRONNEMENT S. A. (type O342M)

9 ⁱGerbig et al., (1999).

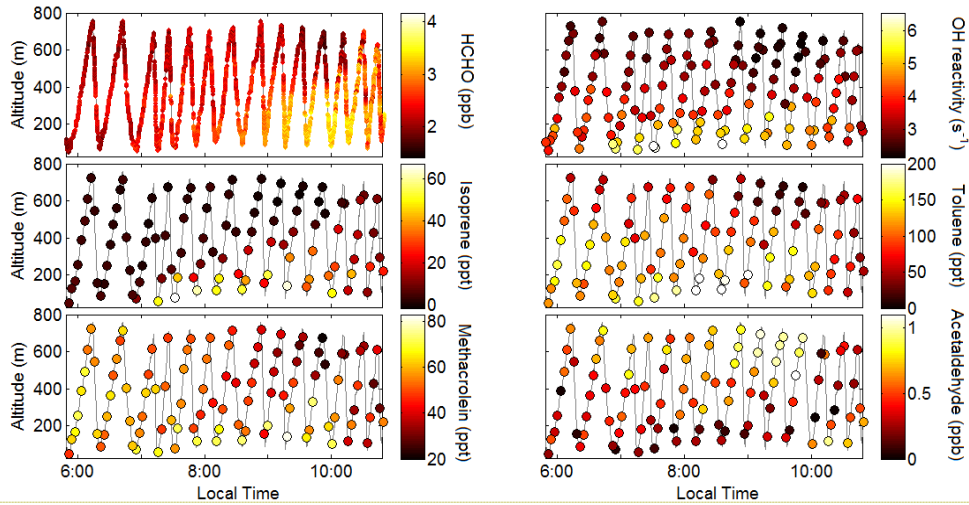
10 ^jGas chromatography/mass spectrometry (Jäger, 2014).

11 ^kBohn et al. (2008). [Accuracy and precision are dependent on conditions and photolysis process.](#)

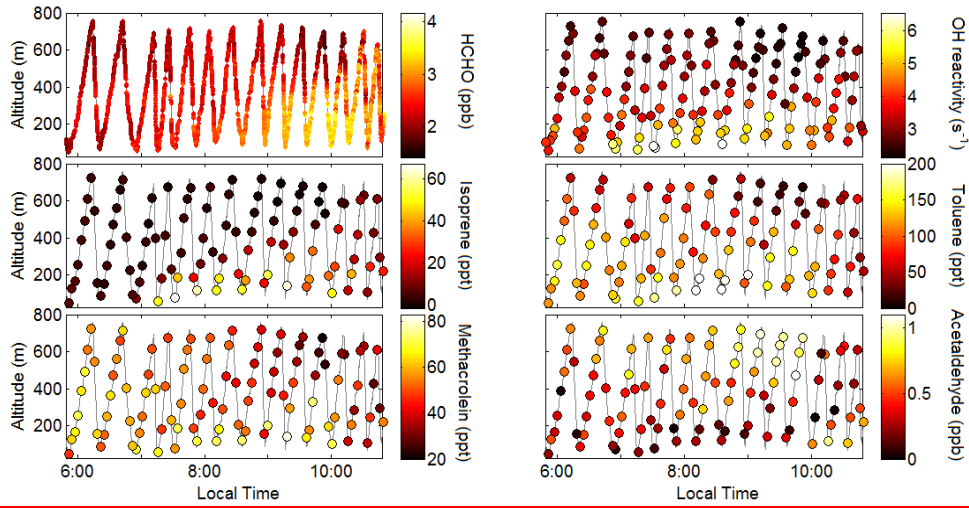
12 [The 15% accuracy is a conservative estimate covering important photolysis frequencies.](#)



1
2 Figure 1. (a) Po Basin, with July 12, 2012 flight track shown in the box and enlarged in (b). (c)
3 Zeppelin altitude during flight.
4



Formatted: Font: 20.5 pt, Font color: Auto



Formatted: Font: 20.5 pt, Font color: Auto

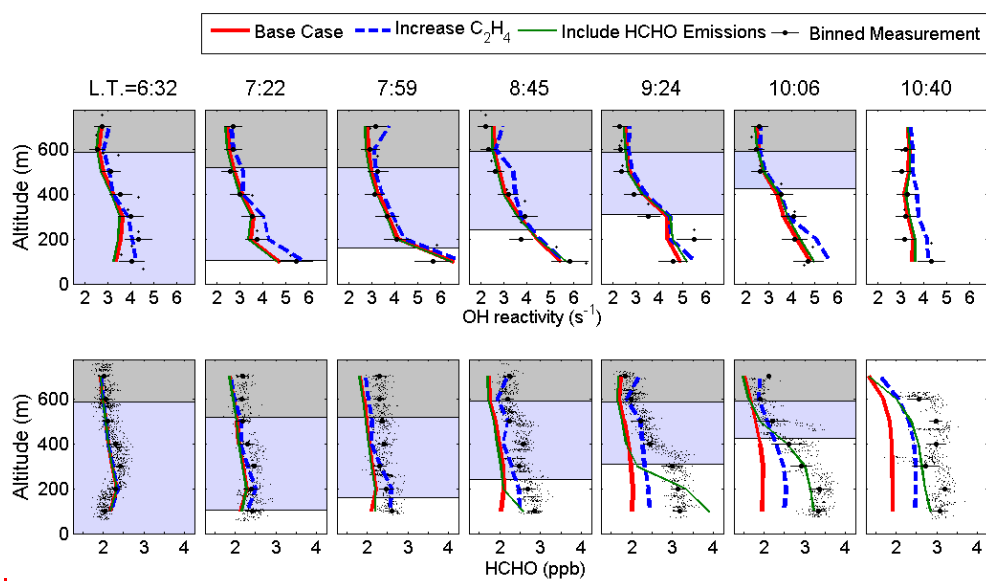
Figure 2. Flight pattern colored by ~~seleets~~selected measurements.

Formatted: Font: 20.5 pt

1

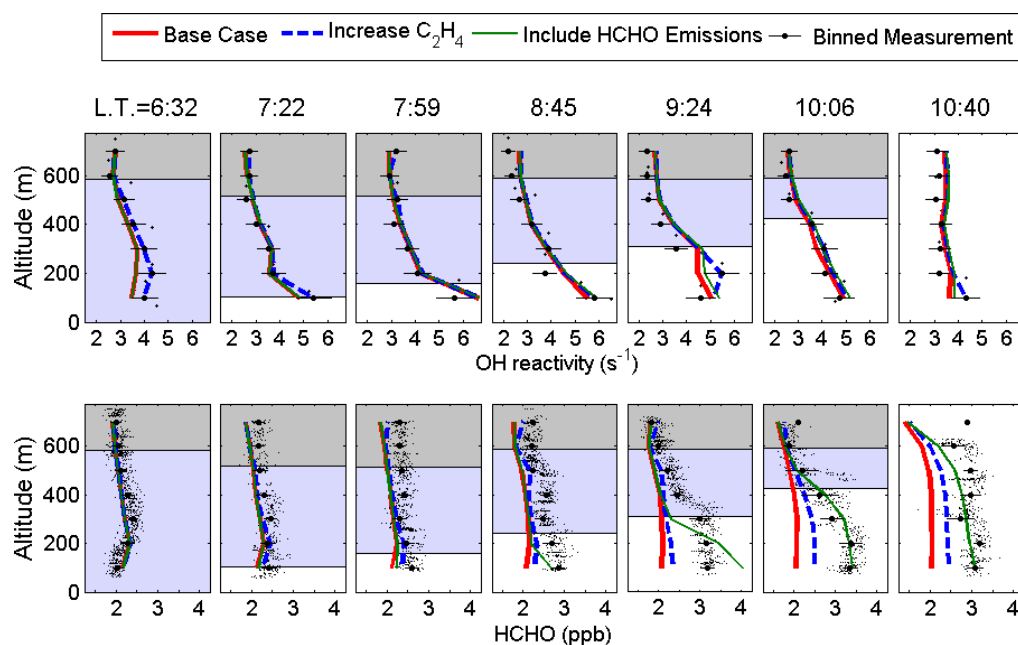
2

3



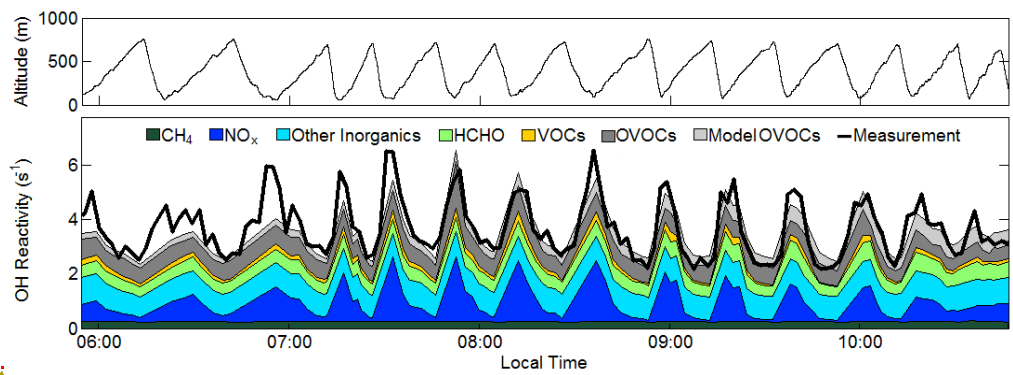
4

Formatted: Font: 20.5 pt, Font color: Auto



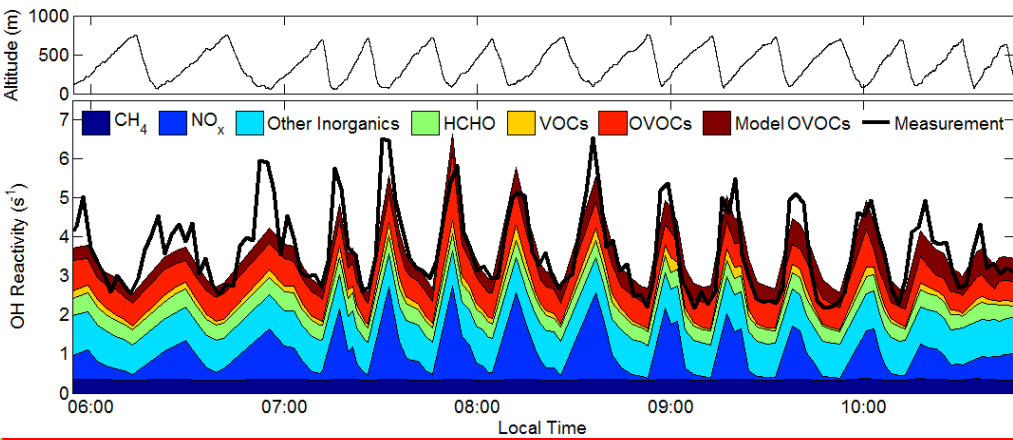
1
 2 Figure 3. Measured and calculated OH reactivity and HCHO vertical profiles for every other
 3 Zeppelin ascent. Error bars on OH reactivity represent the measurement precision. Error bars on
 4 HCHO represent the standard deviation of the measurements in the given altitude bin. The gray,
 5 blue, and white areas represent the residual layer, the nocturnal boundary layer, and the mixed
 6 layer, respectively. Layer height was determined by the observed steep gradients in O₃ mixing
 7 ratios, as detailed in Li et al. (2014). [Model scenarios are described in more detail in sections 3.2](#)
 8 [and 3.3.](#)

1
2
3
4
5
6
7



Formatted: Font: 20.5 pt, Font color: Auto

8

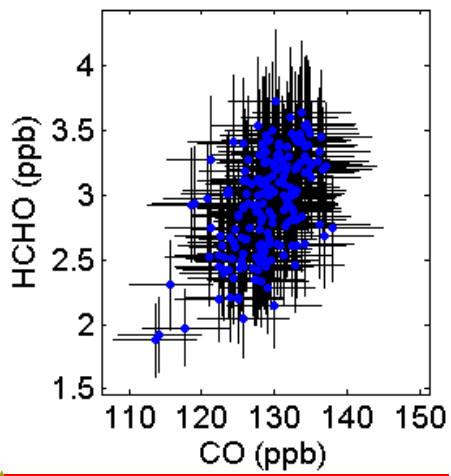


Formatted: Font: 20.5 pt, Font color: Auto

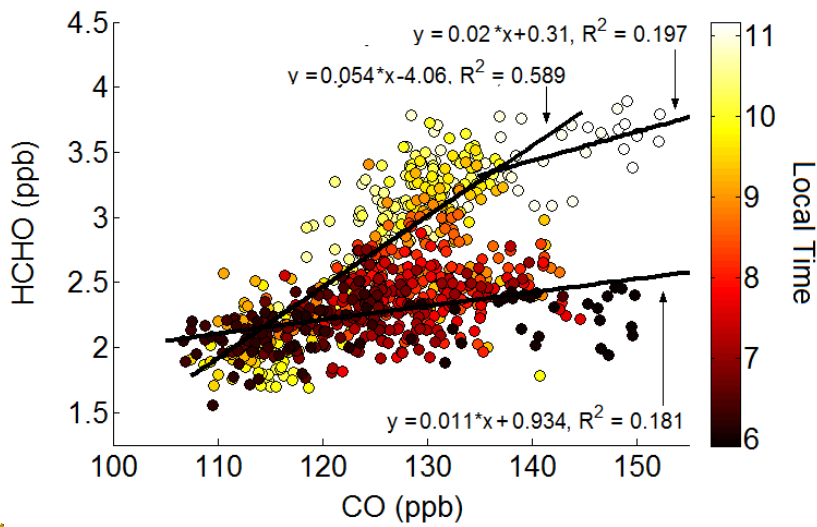
9

10 Figure 4. Contributions to calculated OH reactivity as a function of time. Only data acquired
11 during the ascents is used in the calculated reactivity. The VOC category consists of isoprene,
12 toluene, benzene, xylenes, ethylbenzene, C4-C9 straight chain alkanes, styrene,

1 trimethylbenzene, 1-pentene, cis-2-pentene, cyclohexanone, propylbenzene, isopropylbenzene,
2 isopentane, benzaldehyde, and 1-butene. The OVOC category consists of C2-C6 straight chain
3 aldehydes, acetone, methanol, ethanol, methyl acetate, ethyl acetate, methacrolein, methyl ethyl
4 ketone, methyl vinyl ketone, and 1-propanol. The inorganics category consists of CO, H₂,
5 HONO, HO₂ and O₃. Model OVOCs are non-measured oxidation products calculated by the
6 | MCM.



Formatted: Font color: Auto

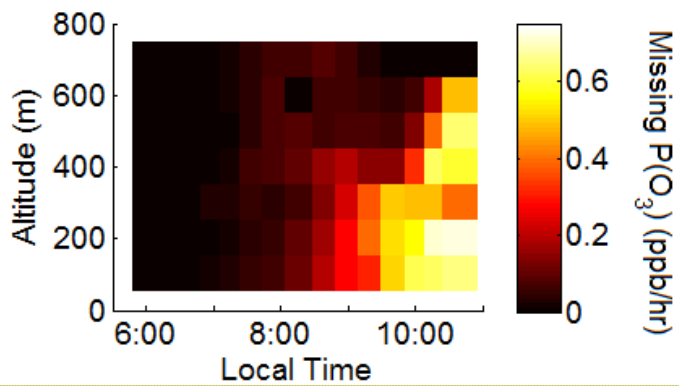


Formatted: Font: 9 pt

Figure 5. Correlation of measured HCHO and CO as a function of time. Linear fits are applied to data acquired before 8:00 (bottom), between 8:00 and 11:00 (middle), and after 11:00 (top).

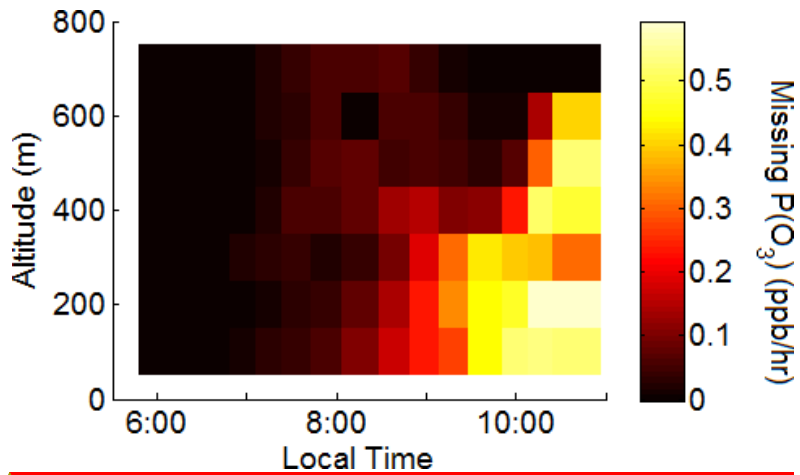
- 1 | Figure 5. HCHO and CO in the mixed layer. Error bars represent instrument accuracy. There is
- 2 | little variation in mixed layer CO, and the correlation with HCHO is small ($r^2 = 0.29$).

1
2
3
4
5



Formatted: Font: 20.5 pt, Font color: Auto

6



Formatted: Font: 20.5 pt, Font color: Auto

7

8 Figure 6. Difference/Underestimate in model ozone production rates using HO₂ mixing ratios/rate
9 caused by the modeled underestimate in HCHO as a function of time and altitude. Missing P(O₃)
10 is defined as P(O₃) calculated ~~when using measured~~ HCHO ~~is~~ minus P(O₃) calculated ~~and~~
11 constrained to measurements. ~~using modeled HCHO.~~